TRIM69 suppressed the anoikis resistance and metastasis of gastric cancer through ubiquitin–proteasome-mediated degradation of PRKCD

Tongguo Shi (shitg@suda.edu.cn)
The First Affiliated Hospital of Soochow University https://orcid.org/0000-0002-5382-2775
Linqing Sun
The First Affiliated Hospital of Soochow University
Yuqi Chen
The First Affiliated Hospital of Soochow University
Lu Xia
The First Affiliated Hospital of Soochow University
Jiayu Wang
The First Affiliated Hospital of Soochow University
Jinghan Zhu
The First Affiliated Hospital of Soochow University
Juntao Li
Kun Wang
The First Affiliated Hospital of Soochow University
Kanger Shen
The First Affiliated Hospital of Soochow University
Dongze Zhang
The First Affiliated Hospital of Soochow University
Guangbo Zhang
The First Affiliated Hospital of Soochow University
Weichang Chen
Department of Gastroenterology, The First Affiliated Hospital of Soochow University

Article

Keywords: Gastric cancer, TRIM69, anoikis resistance, metastasis, PRKCD/BDNF axis

Posted Date: April 6th, 2023

DOI: https://doi.org/10.21203/rs.3.rs-2775066/v1

Additional Declarations: There is **NO** conflict of interest to disclose.

Version of Record: A version of this preprint was published at Oncogene on October 20th, 2023. See the published version at https://doi.org/10.1038/s41388-023-02873-6.

Abstract

The tripartite motif (TRIM) protein family has been investigated in multiple human cancers, including gastric cancer (GC). However, the role of TRIM69 in the anoikis resistance and metastasis of GC cells remains to be elucidated. We identified the differentially expressed genes in anoikis-resistant GC cells using RNA-sequencing analysis. The interaction between TRIM69 and PRKCD was analyzed by coimmunoprecipitation and mass spectrometry. Our results have shown that TRIM69 was significantly downregulated in anoikis-resistant GC cells. TRIM69 overexpression markedly suppressed the anoikis resistance and metastasis of GC cells in *vitro* and in *vivo*. TRIM69 knockdown had the opposite effects. Mechanistically, TRIM69 interacted with PRKCD through its B-box domain and catalyzed the K48-linked polyubiquitination of PRKCD. Moreover, TRIM69 inhibited BDNF production in a PRKCD-dependent manner. Importantly, overexpression of PRKCD or BDNF blocked the effects of TRIM69 on the anoikis resistance and metastasis of GC cells. Interestingly, a $TRIM69^{-}PRKCD^{+}BDNF^{+}$ cell subset was positively associated with metastasis in GC patients. TRIM69-mediated suppression of the anoikis resistance and metastasis of GC cells via modulation of the PRKCD/BDNF axis, with potential implications for novel therapeutic approaches for metastatic GC.

Introduction

Gastric cancer (GC) is a malignancy of the digestive system with the highest mortality rate worldwide[1]. The high rate of metastasis is the major reason for the poor prognosis of patients with GC[2]. Therefore, the identification of key targets and characterization of their molecular mechanisms involved in GC metastasis would contribute to the development of new treatment options.

Tumor metastasis is a multistep biological process in which cancer cells disperse from a primary site; cross the basement membrane (BM), the extracellular matrix (ECM) and vessel walls; and finally colonize distant organs through the blood and lymphatic circulation[3–5]. Anoikis is a form of apoptosis resulting from loss of cell adhesion or adhesion-mediated signaling[6, 7]. It is well known that anoikis resistance (AR) is a necessary condition for the occurrence of tumor metastasis[8, 9]. Previous studies have shown that tumor cells can avoid anoikis by inducing epithelial-mesenchymal transition (EMT), inhibiting apoptotic signaling pathways, changing integrin expression, regulating microRNAs, activating autophagy or inducing oxidative stress[10–15]. Regrettably, the underlying mechanism of anoikis resistance in GC has not been clearly elucidated.

The proteins of the tripartite motif (TRIM) family, a large group of E3 ubiquitin ligases, are characterized by the presence of a RING finger domain, a B-box domain, a coiled-coil region, and a variable C-terminal region[16]. Recently, the TRIM family emerged as a potentially important regulator of various functions in cellular processes, including anoikis resistance pathways[17, 18]. TRIM69 is a member of the TRIM family, and it not only has been reported to function in the defense against viral infections[19, 20] but also has been identified to be closely related to apoptosis[21, 22]. Rong et al. showed that TRIM69 overexpression attenuated ultraviolet B-induced apoptosis and ROS production by inducing p53

ubiquitination[23]. Another report suggested that TRIM69 inhibited apoptosis and inflammation through ASK1 inactivation in mice with high-fat diet (HFD)-induced hippocampal injury[24]. Unfortunately, no studies have reported the function of TRIM69 in anoikis resistance in GC cells.

In the present study, we aimed to investigate the effects of TRIM69 on anoikis resistance in GC cells (AR GC cells). Here, we report the discovery that TRIM69 expression was low in AR GC cells. Overexpression of TRIM69 promoted the anoikis and inhibited the metastasis of AR GC cells via the ubiquitin–proteasome degradation pathway, which reduced the expression of PRKCD, *in vitro* and *in vivo*. In addition, TRIM69 downregulated BDNF expression through PRKCD-mediated signaling pathways. Importantly, we found that low expression of TRIM69 contributed to distant metastasis by analysis of clinical specimens. Thus, our results offer novel mechanistic insight into the distant metastasis of GC and provide a resource for future studies focused on GC pathogenesis or the discovery of therapeutic targets.

Results

TRIM69 expression was low in anoikis-resistant GC cells

To explore the mechanism of anoikis resistance in GC cells, we first established anoikis-resistant (AR) AGS and MKN45 cells. As shown in (Supplementary Fig. 1A), the number of surviving cells was significantly increased in the AR AGS and MKN45 cell groups compared with the control cell groups under detachment conditions. The levels of cleaved caspase3 and cleaved PARP were markedly decreased in AR AGS and MKN45 cells in response to detachment (Supplementary Fig. 1B). The apoptosis rate of AR AGS and MKN45 cells was obviously reduced after culture under detachment conditions (Supplementary Fig. 1C). The acquisition of anoikis resistance is of crucial importance for the survival of cancer cells in a stressful microenvironment[25]. As shown in (Supplementary Fig. 1D), the numbers of colonies of AR AGS and MKN45 cells were greater than those of WT AGS and MKN45 cells under low-serum conditions. Moreover, the migration and invasion abilities of AR AGS and MKN45 cells were significantly enhanced compared with those of control cells (Supplementary Fig. 1E). These results suggested that we successfully established anoikis-resistant GC cells.

Next, we performed RNA-seq analysis to analyze the transcriptomic differences between WT MKN45 cells and AR MKN45 cells. As shown in Fig. 1A and 1B, there were 457 upregulated genes and 119 downregulated genes in AR MKN45 cells compared to WT MKN45 cells. Among these, 17 DEGs meeting the logarithmic fold change criteria (logFC > 4 and logFC < -3.4) were identified (Fig. 1C). Moreover, RT–qPCR was performed to validate the results of the RNA-seq analysis, and the results showed that consistent with the RNA-seq results, WBP2NL, SERPINA1, and PIP5K1B expression levels were increased but FOX1, TRIM69, and GABRR2 expression levels were decreased in AR AGS and MKN45 cells compared to the corresponding control cells (Fig. 1D). Among these downregulated genes, TRIM69, an E3 ubiquitin ligase, attracted our attention. Both the mRNA and protein levels of TRIM69 were lower in AR GC cells (AGS, MKN28, MKN45 and HGC27) than in WT GC cells (Fig. 1E, F).

TRIM69 suppressed the anoikis resistance and metastasis of GC cells in vitro **and** in vivo

To investigate the role of TRIM69 in the anoikis resistance and metastasis of GC cells, we generated GC cells stably overexpressing TRIM69 using AR GC cells (Fig. 2A). TRIM69 overexpression markedly increased caspase-3 and PARP cleavage as well as the apoptosis rate in AR AGS, MKN28, MKN45 and HGC27 cells under detachment conditions (Fig. 2A, B and Supplementary Fig. 2). Additionally, overexpression of TRIM69 led to a decrease in the survival rate of AR GC cells (Fig. 2C). Using a colony formation assay, we observed that all TRIM69-overexpressing clones had lower growth rates than the corresponding controls under low-serum conditions (Fig. 2D). Moreover, compared with those of scrambled control cells, the migration and invasion abilities of TRIM69-overexpressing AR GC cells were obviously decreased (Fig. 2E). To further substantiate the regulatory effect of TRIM69 overexpression on tumor metastasis *in vivo*, we performed a lung metastasis assay in nude mice using MKN28 cells injected via the tail vein. The results showed that the numbers of metastatic nodules in the lungs of mice in the TRIM69 overexpression group were significantly less than those in the control group (Fig. 2F).

Complementary loss-of-function studies were performed to further examine the effect of TRIM69 on the anoikis resistance and metastasis of GC cells. We used three nonoverlapping siRNAs targeting TRIM69 (TRIM69 siRNA-001, siRNA-002 and siRNA-003) to knock down TRIM69 expression in AGS, MKN28 and MKN45 cells (Supplementary Fig. 3A). TRIM69 siRNA-002 and siRNA-003 were selected for further studies. TRIM69 silencing resulted in decreases in the levels of apoptosis-related proteins (cleaved caspase3 and cleaved PARP) and the apoptosis rate in AR AGS, MKN28, and MKN45 cells under detachment conditions (Supplementary Fig. 3B and Fig. 4A, B). The trypan blue exclusion assay showed that knocking down TRIM69 significantly increased the survival rate of GC cells in response to detachment (Supplementary Fig. 4C). In addition, TRIM69 depletion increased the proliferation rate of AGS, MKN28 and MKN45 cells under low-serum conditions (Supplementary Fig. 4D, E). Furthermore, transfection with TRIM69 siRNA-002 and siRNA-003 markedly enhanced the migration and invasion of GC cells (Supplementary Fig. 4F). These results suggest that TRIM69 is an important regulator of anoikis resistance and metastasis in GC cells.

Trim69 Directly Degrades Prkcd Via The Ubiquitin–proteasome Pathway

To explore the potential mechanism by which TRIM69 suppresses the anoikis resistance and metastasis of GC cells, co-IP and LC–MS/MS were conducted to identify potential substrates of TRIM69 related to apoptosis (Fig. 3A). PRKCD, a member of the novel PKC subfamily, has been demonstrated to be closely associated with the apoptotic process[26, 27] (Fig. 3B). Co-IP assays showed that TRIM69 was able to interact with PRKCD in GC cells (Fig. 3C). Similarly, endogenous PRKCD coimmunoprecipitated with exogenous TRIM69 in GC cells (Fig. 3D). Moreover, the interaction between exogenous TRIM69 and PRKCD was demonstrated in HEK293T cells (Fig. 3E). To further explore the functional domains involved in the TRIM69-PRKCD interaction, we constructed several truncations of TRIM69 and PRKCD. As shown

in Fig. 3F, four TRIM69 truncation mutants lacking the RING domain (ΔRING), B-box domain (ΔB-box), Coiled-coil domain (ΔCoiled-coil), or B30.2 domain (ΔB30.2) were constructed[21]. The results of the co-IP assay showed that the B-box domain of TRIM69 interacted with PRCKD (Fig. 3G). In addition, we generated three PRKCD truncation mutants lacking the C2 domain (ΔC2), C1 domain (ΔC1), or protein kinase domain (ΔPKD) (Fig. 3H). As shown in Fig. 3I, we found that the C1 domain of PRKCD interacted with TRIM69.

Considering that TRIM69 is an E3 ligase, we hypothesized that TRIM69 can regulate the protein stability of PRKCD through ubiquitination[21]. The western blot results showed that TRIM69 overexpression markedly decreased the PRKCD protein level (Fig. 4A and Supplementary Fig. 5A). In the presence of the protein synthesis inhibitor cycloheximide (CHX), the half-life of the PRKCD protein in TRIM69-overexpressing cells was much shorter than that in control cells (Fig. 4B). Then, we determined which degradation system predominantly regulates the TRIM69-mediated degradation of PRKCD. Treatment with the ubiquitin–proteasome system inhibitor MG132 rescued TRIM69 overexpression-mediated PRKCD degradation in AGS, MKN28, MKN45 and HGC27 cells (Fig. 4C and Supplementary Fig. 5B). Moreover, TRIM69 overexpression led to accumulation of ubiquitinated PRKCD in the presence of MG132 (Fig. 4D). To determine which lysine (K)-linked polyubiquitin chains are conjugated to PRKCD, we overexpressed several ubiquitin mutants, in which the K48 ubiquitin construct lacked all lysine residues except K48, while the K63 construct lacked all lysine residues except K63. The results of co-IP showed that K48- and K63-linked ubiquitination were the primary types of ubiquitination of PRKCD mediated by TRIM69 (Fig. 4E, F). Altogether, these data demonstrated that TRIM69 acted as a negative regulator of PRKCD protein expression and destabilized PRKCD by enhancing its ubiquitination and degradation.

Prkcd Is Required For Trim69 To Suppress The Anoikis Resistance And Metastasis Of Gc Cells

To investigate whether TRIM69 inhibits GC anoikis resistance and metastasis through PRKCD, we cotransfected the TRIM69 and PRKCD expression plasmids into AR AGS and MKN28 cells (Fig. 5A). PRKCD overexpression significantly decreased the cleavage of caspase3 and PARP in AR GC cells, which was increased in AR GC cells after transfection with the TRIM69 expression plasmid (Fig. 5A and Supplementary Fig. 6A). Moreover, PRKCD overexpression partially reversed the effects of TRIM69 overexpression on the apoptosis, survival, and growth rates (Fig. 5B-D). Additionally, overexpression of TRIM69 markedly decreased the migration and invasion of AR GC cells, and this decrease was reversed by PRKCD overexpression (Fig. 5E, F). Importantly, the *in vivo* lung metastasis assay showed that PRKCD overexpression abolished the inhibitory effect of TRIM69 on the lung metastatic ability of AR GC cells (Fig. 5G and Supplementary Fig. 6B). In conclusion, these results demonstrated that TRIM69 negatively regulated GC anoikis resistance and metastasis through PRKCD.

The TRIM69/PRKCD axis inhibits anoikis resistance and metastasis via BDNF in GC cells

Cytokines are key proteins in signaling in the tumor microenvironment (TME) that have pleiotropic effects and are associated with cancer progression, invasion, and metastasis[28–30]. Therefore, we explored whether TRIM69 modulates anoikis resistance and metastasis via one or more cytokines. A Human Cytokine Array G5 was employed to identify differentially expressed cytokines between OE-NC and OE-TRIM69 MKN45 cells. The results showed that 12 cytokines were downregulated and 29 were upregulated (Fig. 6A, B). Figure 6C shows the top 3 downregulated (MCP-1, BDNF, and NAP-2) and upregulated (TNFRSF11B, IGFBP-3, and IL-16) cytokines. Previous studies have shown that BDNF/TrkB is related to anoikis resistance, tumor progression and poor prognosis in many types of malignancies[31–33]. Therefore, we inferred that BDNF might be involved in the TRIM69-mediated regulation of anoikis resistance and metastasis. The ELISA data showed that the level of BDNF was lower in the OE-TRIM69 group than in the OE-NC group (Fig. 6D). Similar results were also found by RT—qPCR and western blot analysis (Fig. 6E, F and Supplementary Fig. 7A). Furthermore, PRKCD overexpression reversed the effects of TRIM69 overexpression on the mRNA and protein expression of BDNF in AR AGS and MKN28 cells (Fig. 6G-I and Supplementary Fig. 7B). These results suggested that TRIM69 inhibited BDNF expression in GC cells in a PRCKD-dependent manner.

We next verified whether BDNF is involved in the TRIM69-mediated anoikis resistance and metastasis of GC cells. As shown in Fig. 6J, supplementation with human recombinant BDNF (hr BDNF) reduced the levels of cleaved caspase-3 and cleaved PARP in AR GC cells, which were increased after TRIM69 overexpression (Supplementary Fig. 7C). Moreover, addition of hr BDNF reversed the effects of TRIM69 on the apoptosis and survival rates of AR GC cells (Fig. 6K, L). Additionally, treatment with hr BDNF abolished the TRIM69 overexpression-induced decrease in cell growth under low-serum conditions as well as the decreases in the migration and invasion abilities of AR GC cells (Fig. 6M, N). Altogether, these findings indicate that the roles of the TRIM69/PRCKD axis in preventing anoikis resistance and metastasis are dependent on BDNF.

The Proportion Of Trim69prkcdbdnf Cells Was Positively Associated With Metastasis In Gc Patients

To analyze the associations between TRIM69, PRKCD and BDNF expression and metastasis in GC patients, an mIHC assay was performed. As shown in Fig. 7A and 7B, compared with that in nonmetastatic (M0) tissues, the expression of TRIM69 in metastatic GC (M1) tissues was significantly decreased in the epithelial region. Importantly, low TRIM69 expression ($TRIM69^{-}$) was significantly positively correlated with pathologic differentiation ($P = 0.047$), more advanced clinical stage ($P = 0.044$), and distant metastasis ($P = 0.007$), as shown in (Supplementary Table 1). Moreover, we examined PRKCD and BDNF protein expression in tissue samples from patients with GC (Fig. 7A). As shown in Fig. 7B, the expression of PRKCD was markedly increased in M1 tissues compared with M0 tissues. However, there was no difference in BDNF expression between M0 and M1 tissues (Fig. 7B). Interestingly, we observed that tumors in patients with high proportions of $TRIM69^{-}PRKCD^{+}$, $TRIM69^{-}BDNF^{+}$, $PRKCD^{+}BDNF^{+}$ and $TRIM69^{-}PRKCD^{+}BDNF^{+}$ tumor cell subsets showed higher metastatic potential (Fig. 7C, D).

Discussion

Anoikis resistance is essential for tumor metastasis, allows tumor cells to survive during circulation in the bloodstream and facilitates their metastasis to distant organs[34, 35]. However, the underlying molecular mechanism of anoikis resistance in GC remains unclear. In the present study, we established a model of anoikis resistance in GC cells *in vitro* and found that TRIM69 expression was significantly downregulated in anoikis-resistant GC cells. TRIM69 is a RING finger domain-containing E3 ligase that belongs to the tripartite motif (TRIM) family. It was initially discovered in a human testis cDNA library and can mediate ubiquitination *in vivo*, playing a very important role in the process of spermatogenesis and participating in apoptosis[21, 23]. However, the molecular function of TRIM69 has not been extensively studied in various types of cancer cells. In this study, we confirmed that TRIM69 overexpression inhibited but TRIM69 knockdown promoted the anoikis resistance, migration and invasion of GC cells *in vitro*. Moreover, TRIM69 overexpression impaired distant metastasis *in vivo*. In addition, TRIM69 was expressed at low levels in metastatic GC tissues, and TRIM69 expression was negatively associated with distant metastasis. Although the mechanism by which TRIM69 is downregulated in anoikis-resistant GC cells remains unknown and needs further investigation, our data demonstrated a crucial role for TRIM69 in regulating anoikis resistance and metastasis in GC.

PRKCD is a member of the protein kinase C family of serine- and threonine-specific protein kinases[36, 37] and is involved in the progression of GC[38, 39]. For example, PRKCD overexpression enhances the metastasis, chemoresistance, and stem cell-like characteristics of GC cells[38]. Yoshihiko Iioka et al. noted that PRKCD, in cooperation with p53, modulates cisplatin-induced caspase-3-mediated cell death in GC[39]. In the current study, the results of co-IP and LC–MS/MS analysis showed that TRIM69 might interact directly with the PRKCD protein in GC cells. Importantly, PRKCD expression was regulated by TRIM69-mediated ubiquitination. Moreover, the results of the mutagenesis and co-IP assays showed that the ubiquitination of PRKCD induced by TRIM69 was both K48- and K63-linked, which are commonly observed types of ubiquitination. These results were consistent with a previous study reported by Han et al.[21]. K48-linked polyubiquitination of target proteins leads to proteasome-mediated degradation, while K63-linked ubiquitination has been implicated in the activation of several signaling pathways. Furthermore, K63-linked polyubiquitination has been shown to promote protein degradation through the autophagy pathway[40, 41]. We cannot explain the K63-linked polyubiquitination-mediated degradation of PRKCD in GC cells under autophagic conditions observed in the present study. Further investigations are required to explain this phenomenon. More importantly, the rescue experiment showed that PRKCD overexpression abolished the effect of TRIM69 on GC cell anoikis resistance and metastasis *in vitro* and *in vivo*. Overall, we arrived at the novel conclusion that TRIM69 destabilizes PRKCD by enhancing its ubiquitination and degradation and suppresses the anoikis resistance and metastasis of GC cells through this effect on PRKCD.

BDNF is a member of the nerve growth factor family of proteins and participates in cellular differentiation, proliferation, and survival processes in the nervous system[42–44]. A number of studies have noted that BDNF plays crucial roles in the progression of various cancers, including GC[45–47]. For

instance, lactate/BDNF/TrkB signaling is involved in the crosstalk between tumor cells and activated fibroblasts and enhances anlotinib resistance in GC[48]. Ding et al. reported that BDNF expression was upregulated in GC tissues and that BDNF knockdown inhibited the proliferation, migration and invasion of GC cells[49]. In this study, BDNF was significantly downregulated in TRIM69-overexpressing GC cells. PRKCD overexpression reversed the effect of TRIM69 overexpression on BDNF expression. A previous study showed that PRKCD activation upregulated BDNF expression in retinal ganglion cells[37]. These results indicate that TRIM69 negatively regulates BDNF expression in GC cells via PRKCD. However, the precise mechanism by which TRIM69/PRCKD signaling regulates BDNF expression is still unclear. Hence, we will further explore the mechanism by which TRIM69/PRCKD signaling regulates BDNF expression in our next study. Importantly, hr BDNF abolished the effects of TRIM69 on the anoikis resistance and metastasis of GC cells. Collectively, our findings indicated that the TRIM69/PRCKD axis modulated the anoikis resistance and metastasis of GC cells through BDNF. Importantly, we also identified a $TRIM69^{-}PRKCD^{+}BDNF^{+}$ tumor cell subset, whose presence was positively correlated with distant metastasis in GC patients.

Conclusions

In summary, we investigated the novel role of TRIM69 in anoikis resistance and metastasis in GC and revealed a new mechanism for the regulation of PRKCD expression by TRIM69-mediated ubiquitination and degradation. Furthermore, TRIM69/PRCKD signaling was found to suppress anoikis resistance and metastasis by inhibiting BDNF expression (Fig. 8). Hence, it is of great value to develop therapeutic approaches targeting TRIM69 or blocking PRCKD/BDNF as potential GC interventions.

Materials And Methods

Patients and specimens

GC tissue microarray (TMA) chips, which contained 162 pairs of GC tissue samples and adjacent normal tissues, as well as follow-up data, were obtained from Shanghai Outdo Biotech Co., Ltd. (Shanghai, China). The relevant clinical data for each patient were collected and are provided in (Supplementary Table 2). Additionally, we obtained approval for this study from the Ethics Review Board of the First Affiliated Hospital of Soochow University (Approval number: 2022 – 117).

Western Blotting

Western blot analysis was performed as previously reported[50]. Briefly, cells were lysed with IP buffer (Beyotime, Shanghai, China) supplemented with protease inhibitors (NCM, Suzhou, China). Protein concentrations were examined with an Enhanced BCA Protein Assay Kit (Beyotime, Shanghai, China). Total protein (30 μg) was separated by sodium dodecyl sulfate–polyacrylamide gel electrophoresis (SDS–PAGE, NCM, Suzhou, China) and transferred onto polyvinylidene fluoride (PVDF) membranes (GE

Healthcare Life Science, Germany). The membranes were blocked for 1.5 h at room temperature using 5% (w/v) skim milk powder in TBST (Beyotime, Shanghai, China) and were then incubated with the primary antibody overnight in antibody diluent at 4°C (NCM, Suzhou, China). On the following day, the membranes were incubated with the corresponding HRP-conjugated goat anti-rabbit or anti-mouse secondary antibody for 1 h at room temperature. The protein bands were visualized with ECL reagents (NCM, Suzhou, China) in a ChemiDocTM MP Imaging System (Bio-Rad, CA, USA). The band density was analyzed using ImageJ software (RRID:SCR_003070). All antibodies used in this study and the corresponding vendors are listed in (Supplementary Table 3).

Anoikis Assay

Poly-2-hydroxyethyl methacrylate (poly-HEMA, Sigma—Aldrich) was prepared by solubilization in anhydrous ethanol (v/v) to a concentration of 10 mg/ml. To induce anoikis, 1 ml of the poly-HEMA solution was added to 6-well plates overnight at room temperature. Then, 1×10^6 cells were grown in poly-HEMA-coated 6-well plates for 48 h. Finally, cells in suspension were collected and used for western blot analysis, a trypan blue exclusion assay, and an apoptosis assay.

Apoptosis Assay

The apoptosis assay was conducted as previously described[50]. Briefly, equal numbers of GC cells cultured in poly-HEMA-coated 6-well plates were collected and stained with Annexin V-PE and 7-AAD (BD Biosciences, USA) according to the manufacturer's instructions. Then, apoptosis was immediately analyzed using a flow cytometer (FACS Aria, Beckman Coulter, Brea, CA, USA). The apoptosis rate was determined using FlowJo software (RRID: SCR_008520).

Cell Migration And Invasion Assays

To evaluate the migration ability, cells in medium with 1% FBS were seeded in the upper chambers, which contained an 8 μm pore size membrane, of a 24-well plate (Corning, China). To evaluate the invasion ability, the membranes in the upper chambers were coated with 100 μl diluted Matrigel (200 μg/ml, Corning, China) for 2 h. Then, the upper chambers were placed into the bottom chambers, which contained 800 μl of cell culture medium containing 20% FBS. After 24–48 h, the cells were fixed with 4% paraformaldehyde for 30 min and then stained with 1% crystal violet (Beyotime, Shanghai, China) for 30 min. Finally, the cells were counted by light microscopy.

Rna-seq Assay

MKN45 GC cells (1×10^6) were seeded in poly-HEMA-coated 6-well plates. After culture for 24 h, detached MKN45 cells were collected and returned to adherent culture for 24 h. This detachment/attachment cycle

was repeated until the emergence of anoikis resistance for 4 cycles. The cells obtained by the above method were called anoikis-resistant cells (AR MKN45 cells). Total RNA from WT MKN45 and AR MKN45 cells was isolated with TRIzol (Vazyme, Nanjing, China) and analyzed by RiboBio Life Science Co., Ltd. (Guangzhou, China).

Coimmunoprecipitation (Co-ip) Assay

To detect the interaction of endogenous TRIM69 with PRKCD, AGS, MKN28 or MKN45 cell lysates were obtained by using IP lysis buffer (Beyotime, Shanghai, China) and incubated with 2 μg of an anti-PRKCD antibody or anti-rabbit IgG (Beyotime, Shanghai, China) overnight at 4°C. Protein A + G magnetic beads (Beyotime, Shanghai, China) were added to the cell mixtures and incubated for 4 h at 4°C. For the interaction between exogenous TRIM69 and PRKCD, AGS, MKN28, MKN45 or HEK293T cells were transfected with TRIM69 or PRKCD plasmids. After culture for 48 h, the cells were homogenized in lysis buffer for immunoprecipitation (Beyotime, Shanghai, China). Then, the cell lysates were incubated with 20 μl of anti-IgG magnetic beads (Beyotime, Shanghai, China) overnight at 4°C. The next day, the mixtures were incubated with anti-Flag, anti-HA or anti-Myc magnetic beads (Beyotime, Shanghai, China) for 4 h at 4°C. After the beads were washed four times with lysis buffer for IP, the precipitates were collected, and proteins were eluted with 1×SDS sample buffer. The samples were analyzed using western blotting.

Liquid Chromatography–mass Spectrometry (Lc–ms/ms)

MKN45 cells were transfected with Flag-TRIM69 plasmids, lysed with IP lysis buffer and immunoprecipitated using anti-Flag magnetic beads (Beyotime, Shanghai, China). After the beads were washed four times with IP lysis buffer, the eluted proteins were separated by SDS–PAGE and stained with Coomassie blue. Then, the protein bands were excised from the gel and subjected to reduction and tryptic digestion. Peptide sequences were determined by a Q EXACTIVE mass spectrometer (Thermo Fisher) at Suzhou BioNovoGene Biomedical Tech Co., Ltd. (Suzhou, China). Protein identification was performed with MaxQuant 1.5.5.1 software by comparison against the UniProtKB/Swiss-Prot Human database [UniProtKB/Swiss-Prot Release 2012_12].

Tumor metastasis in vivo

Six- to eight-week-old female BALB/c athymic nude mice were purchased from the Shanghai Laboratory Animal Center. All animal experiments were approved by the Institutional Animal Care and Use Committee of Soochow University (Suzhou, China) (Ethical number, 202206A0710). For the lung metastasis model, single-cell suspensions of 3×10^6 cells were injected into the tail veins of nude mice. The mice were killed 8 weeks after injection, the lungs were resected and fixed with paraformaldehyde, and the visible tumor nodules were counted. The fixed lungs were then embedded in paraffin, sectioned, and stained with hematoxylin and eosin, and microscopic lung metastases were counted by light microscopy.

Mihc Assay

mIHC was performed using an Opal 7-Color Manual IHC Kit (PerkinElmer Inc., USA), as previously described[51, 52]. Briefly, slides were labeled with four antibodies, namely, anti-TRIM69 (1:100), anti-PRKCD (1:500), anti-BDNF (1:500), and anti-CK (1:5), prior to incubation with the corresponding HRP-conjugated secondary antibody (Genetech, China). An appropriate Opal fluorophore-conjugated TSA (PerkinElmer, USA) was then added at a 1:100 dilution. After each step, the slides were rinsed with TBST. Microwave treatment was used to remove the antibody–TSA complexes after every staining cycle, staining with the next marker was then performed until all four markers were labeled, and finally, spectral 4′,6-diamidino-2-phenylindole (DAPI) (PerkinElmer, USA) was added. The slides were mounted with VECTASHIELD® HardSet Antifade Mounting Medium (Vector Labs). Panoramic image acquisition was performed using a TissueFAXS SPECTRA multispectral panoramic tissue scanning quantitative analysis system. Spectral channel resolution was performed using TissueFAXS analysis software. DAPI channels were used to locate and identify nuclei and to identify and quantitatively analyze cells with positive cytoplasmic staining.

Other Methods

Detailed descriptions of other methods used in this study are provided in Supplementary Materials and Methods.

Statistical analysis

All statistical data were analyzed with GraphPad Prism 9.0 (La Jolla, CA, USA), and the data are presented as the means ± SD (SEM). Student's *t* test was used to analyze differences between two groups. A one-way ANOVA test was used for multiple comparisons. The relationships between clinical parameters and indicates gene expression were determined by using two-sided Chi-square test. All experiments were performed in triplicate, and $P < 0.05$ was considered statistically significant.

Declarations

Data availability

The data supporting this study's findings are available from the corresponding author upon reasonable request.

Acknowledgements

This work was supported by The National Natural Science Foundation of China (81802843,82073156,82270561,81872328); Key Research and Development Program of Jiangsu Province (BE2020656); The key project of Jiangsu Provincial Health and wellness Commission

(ZD2021050); The Health Personnel Training Project of Suzhou (GSWS201903); Suzhou “Science and Education Revitalize Health” Youth Science and Technology Project (KJXW2022005).

Author contributions

The authors checked and approved the final manuscript. LQS, JYW, and JTL performed the experiments. LQS, YQC, and LX performed the data analysis. KW and KES performed sample collection and clinical evaluation. JHZ and DZZ provided guidance on experimental technology. GBZ, TGS and WCC are the corresponding authors and they designed the research. The manuscript was wrote by LQS and revised by GBZ, TGS, and WCC.

Competing interests

The authors declare that they have no competing interests.

References

1. Bray F, Ferlay J, Soerjomataram I, Siegel R, Torre L, Jemal A. Global cancer statistics 2018: GLOBOCAN estimates of incidence and mortality worldwide for 36 cancers in 185 countries. CA: a cancer journal for clinicians 2018; 68: 394–424.
2. Shao S, Yang X, Zhang Y, Wang X, Li K, Zhao Y *et al*. Oncolytic Virotherapy in Peritoneal Metastasis Gastric Cancer: The Challenges and Achievements. Frontiers in molecular biosciences 2022; 9: 835300.
3. Zhang T, Wu Y, Fang Z, Yan Q, Zhang S, Sun R *et al*. Low expression of RBMS3 and SFRP1 are associated with poor prognosis in patients with gastric cancer. American journal of cancer research 2016; 6: 2679–2689.
4. Mahdikia H, Saadati F, Freund E, Gaipl U, Majidzadeh-A K, Shokri B *et al*. Gas plasma irradiation of breast cancers promotes immunogenicity, tumor reduction, and an abscopal effect in vivo. Oncoimmunology 2020; 10: 1859731.
5. Elia I, Broekaert D, Christen S, Boon R, Radaelli E, Orth M *et al*. Proline metabolism supports metastasis formation and could be inhibited to selectively target metastasizing cancer cells. Nature communications 2017; 8: 15267.
6. Jiang K, Chaimov D, Patel S, Liang J, Wiggins S, Samojlik M *et al*. 3-D physiomimetic extracellular matrix hydrogels provide a supportive microenvironment for rodent and human islet culture. Biomaterials 2019; 198: 37–48.
7. Winkler J, Abisoye-Ogunniyan A, Metcalf K, Werb Z. Concepts of extracellular matrix remodelling in tumour progression and metastasis. Nature communications 2020; 11: 5120.
8. Jin L, Chun J, Pan C, Kumar A, Zhang G, Ha Y *et al*. The PLAG1-GDH1 Axis Promotes Anoikis Resistance and Tumor Metastasis through CamKK2-AMPK Signaling in LKB1-Deficient Lung Cancer. Molecular cell 2018; 69: 87–99.e87.

9. Tan Y, Lin K, Zhao Y, Wu Q, Chen D, Wang J *et al*. viaAdipocytes fuel gastric cancer omental metastasis PITPNC1-mediated fatty acid metabolic reprogramming. Theranostics 2018; 8: 5452–5468.
10. Avalle L, Incarnato D, Savino A, Gai M, Marino F, Pensa S *et al*. MicroRNAs-143 and – 145 induce epithelial to mesenchymal transition and modulate the expression of junction proteins. Cell death and differentiation 2017; 24: 1750–1760.
11. Haun F, Neumann S, Peintner L, Wieland K, Habicht J, Schwan C *et al*. Identification of a novel anoikis signalling pathway using the fungal virulence factor gliotoxin. Nature communications 2018; 9: 3524.
12. Gan L, Liu P, Lu H, Chen S, Yang J, McCarthy J *et al*. Cyclin D1 promotes anchorage-independent cell survival by inhibiting FOXO-mediated anoikis. Cell death and differentiation 2009; 16: 1408–1417.
13. Malagobadan S, Ho C, Nagoor N. MicroRNA-6744-5p promotes anoikis in breast cancer and directly targets NAT1 enzyme. Cancer biology & medicine 2020; 17: 101–111.
14. Chen J, David J, Cook-Spaeth D, Casey S, Cohen D, Selvendiran K *et al*. Autophagy Induction Results in Enhanced Anoikis Resistance in Models of Peritoneal Disease. Molecular cancer research: MCR 2017; 15: 26–34.
15. Takahashi N, Chen H, Harris I, Stover D, Selfors L, Bronson R *et al*. Cancer Cells Co-opt the Neuronal Redox-Sensing Channel TRPA1 to Promote Oxidative-Stress Tolerance. Cancer cell 2018; 33: 985–1003.e1007.
16. Maarifi G, Smith N, Maillet S, Moncorgé O, Chamontin C, Edouard J *et al*. TRIM8 is required for virus-induced IFN response in human plasmacytoid dendritic cells. Science advances 2019; 5: eaax3511.
17. Guo P, Qiu Y, Ma X, Li T, Ma X, Zhu L *et al*. Tripartite motif 31 promotes resistance to anoikis of hepatocarcinoma cells through regulation of p53-AMPK axis. Experimental cell research 2018; 368: 59–66.
18. Ma X, Ma X, Qiu Y, Zhu L, Lin Y, You Y *et al*. TRIM50 suppressed hepatocarcinoma progression through directly targeting SNAIL for ubiquitous degradation. Cell death & disease 2018; 9: 608.
19. Rihn S, Aziz M, Stewart D, Hughes J, Turnbull M, Varela M *et al*. TRIM69 Inhibits Vesicular Stomatitis Indiana Virus. Journal of virology 2019; 93.
20. Wang K, Zou C, Wang X, Huang C, Feng T, Pan W *et al*. Interferon-stimulated TRIM69 interrupts dengue virus replication by ubiquitinating viral nonstructural protein 3. PLoS pathogens 2018; 14: e1007287.
21. Han Y, Li R, Gao J, Miao S, Wang L. Characterisation of human RING finger protein TRIM69, a novel testis E3 ubiquitin ligase and its subcellular localisation. Biochemical and biophysical research communications 2012; 429: 6–11.
22. Han R, Wang R, Zhao Q, Han Y, Zong S, Miao S *et al*. Trim69 regulates zebrafish brain development by ap-1 pathway. Scientific reports 2016; 6: 24034.
23. Rong X, Rao J, Li D, Jing Q, Lu Y, Ji Y. TRIM69 inhibits cataractogenesis by negatively regulating p53. Redox biology 2019; 22: 101157.

24. Li L, Zheng J, Kang R, Yan J. Targeting Trim69 alleviates high fat diet (HFD)-induced hippocampal injury in mice by inhibiting apoptosis and inflammation through ASK1 inactivation. Biochemical and biophysical research communications 2019; 515: 658–664.
25. Mak C, Yung M, Hui L, Leung L, Liang R, Chen K *et al*. MicroRNA-141 enhances anoikis resistance in metastatic progression of ovarian cancer through targeting KLF12/Sp1/survivin axis. Molecular cancer 2017; 16: 11.
26. Wang X, Li Y, He M, Kong X, Jiang P, Liu X *et al*. UbiBrowser 2.0: a comprehensive resource for proteome-wide known and predicted ubiquitin ligase/deubiquitinase-substrate interactions in eukaryotic species. Nucleic acids research 2022; 50: D719-D728.
27. Li Y, Xie P, Lu L, Wang J, Diao L, Liu Z *et al*. An integrated bioinformatics platform for investigating the human E3 ubiquitin ligase-substrate interaction network. Nature communications 2017; 8: 347.
28. Zheng X, Wu Y, Bi J, Huang Y, Cheng Y, Li Y *et al*. The use of supercytokines, immunocytokines, engager cytokines, and other synthetic cytokines in immunotherapy. Cellular & molecular immunology 2022; 19: 192–209.
29. Wei J, Gronert K. Eicosanoid and Specialized Proresolving Mediator Regulation of Lymphoid Cells. Trends in biochemical sciences 2019; 44: 214–225.
30. Ren J, Smid M, Iaria J, Salvatori D, van Dam H, Zhu H *et al*. Cancer-associated fibroblast-derived Gremlin 1 promotes breast cancer progression. Breast cancer research: BCR 2019; 21: 109.
31. Akil H, Perraud A, Jauberteau M, Mathonnet M. Tropomyosin-related kinase B/brain derived-neurotrophic factor signaling pathway as a potential therapeutic target for colorectal cancer. World journal of gastroenterology 2016; 22: 490–500.
32. Li T, Yu Y, Song Y, Li X, Lan D, Zhang P *et al*. Activation of BDNF/TrkB pathway promotes prostate cancer progression via induction of epithelial-mesenchymal transition and anoikis resistance. FASEB journal: official publication of the Federation of American Societies for Experimental Biology 2020; 34: 9087–9101.
33. Yuan Y, Ye H, Ren Q. Proliferative role of BDNF/TrkB signaling is associated with anoikis resistance in cervical cancer. Oncology reports 2018; 40: 621–634.
34. Taddei M, Giannoni E, Fiaschi T, Chiarugi P. Anoikis: an emerging hallmark in health and diseases. The Journal of pathology 2012; 226: 380–393.
35. Paoli P, Giannoni E, Chiarugi P. Anoikis molecular pathways and its role in cancer progression. Biochimica et biophysica acta 2013; 1833: 3481–3498.
36. Li S, Huang Q, Zhou D, He B. PRKCD as a potential therapeutic target for chronic obstructive pulmonary disease. International immunopharmacology 2022; 113: 109374.
37. Braga L, Miranda R, Granja M, Giestal-de-Araujo E, Dos Santos A. PKC delta activation increases neonatal rat retinal cells survival in vitro: Involvement of neurotrophins and M1 muscarinic receptors. Biochemical and biophysical research communications 2018; 500: 917–923.
38. Yuan Y, Yangmei Z, Rongrong S, Xiaowu L, Youwei Z, Sun S. Sotrastaurin attenuates the stemness of gastric cancer cells by targeting PKCδ. Biomedicine & pharmacotherapy = Biomedecine &

pharmacotherapie 2019; 117: 109165.

39. Nakashima K, Uekita T, Yano S, Kikuchi J, Nakanishi R, Sakamoto N *et al*. Novel small molecule inhibiting CDCP1-PKCδ pathway reduces tumor metastasis and proliferation. Cancer science 2017; 108: 1049–1057.
40. Nitschke F, Ahonen S, Nitschke S, Mitra S, Minassian B. Lafora disease - from pathogenesis to treatment strategies. Nature reviews Neurology 2018; 14: 606–617.
41. Humphries F, Bergin R, Jackson R, Delagic N, Wang B, Yang S *et al*. The E3 ubiquitin ligase Pellino2 mediates priming of the NLRP3 inflammasome. Nature communications 2018; 9: 1560.
42. Zhai Y, Wang Q, Zhu Z, Hao Y, Han F, Hong J *et al*. High-efficiency brain-targeted intranasal delivery of BDNF mediated by engineered exosomes to promote remyelination. Biomaterials science 2022; 10: 5707–5718.
43. Ibarra I, Ratnu V, Gordillo L, Hwang I, Mariani L, Weinand K *et al*. Comparative chromatin accessibility upon BDNF stimulation delineates neuronal regulatory elements. Molecular systems biology 2022; 18: e10473.
44. Xu J, Xi K, Tang J, Wang J, Tang Y, Wu L *et al*. Engineered Living Oriented Electrospun Fibers Regulate Stem Cell Para-Secretion and Differentiation to Promote Spinal Cord Repair. Advanced healthcare materials 2022: e2202785.
45. Lin X, Dinglin X, Cao S, Zheng S, Wu C, Chen W *et al*. Enhancer-Driven lncRNA BDNF-AS Induces Endocrine Resistance and Malignant Progression of Breast Cancer through the RNH1/TRIM21/mTOR Cascade. Cell reports 2020; 31: 107753.
46. Yap N, Toh Y, Tan C, Acharya M, Chan A. Relationship between cytokines and brain-derived neurotrophic factor (BDNF) in trajectories of cancer-related cognitive impairment. Cytokine 2021; 144: 155556.
47. Esfandi F, Bouraghi H, Glassy M, Taheri M, Kahaei M, Kholghi Oskooei V *et al*. Brain-derived neurotrophic factor downregulation in gastric cancer. Journal of cellular biochemistry 2019; 120: 17831–17837.
48. Jin Z, Lu Y, Wu X, Pan T, Yu Z, Hou J *et al*. The cross-talk between tumor cells and activated fibroblasts mediated by lactate/BDNF/TrkB signaling promotes acquired resistance to anlotinib in human gastric cancer. Redox biology 2021; 46: 102076.
49. Ding D, Hou R, Gao Y, Feng Y. miR-613 inhibits gastric cancer progression through repressing brain derived neurotrophic factor. Experimental and therapeutic medicine 2018; 15: 1735–1741.
50. Li J, Sun L, Chen Y, Zhu J, Shen J, Wang J *et al*. Gastric cancer-derived exosomal miR-135b-5p impairs the function of Vγ9Vδ2 T cells by targeting specificity protein 1. Cancer immunology, immunotherapy: CII 2022; 71: 311–325.
51. Ng H, Lee R, Goh S, Tay I, Lim X, Lee B *et al*. Immunohistochemical scoring of CD38 in the tumor microenvironment predicts responsiveness to anti-PD-1/PD-L1 immunotherapy in hepatocellular carcinoma. *Journal for immunotherapy of cancer* 2020; 8.

52. Seo Y, Jiang X, Sullivan K, Jalikis F, Smythe K, Abbasi A *et al*. Mobilization of CD8 T Cells via CXCR4 Blockade Facilitates PD-1 Checkpoint Therapy in Human Pancreatic Cancer. Clinical cancer research: an official journal of the American Association for Cancer Research 2019; 25: 3934–3945.

Figures

Figure 1

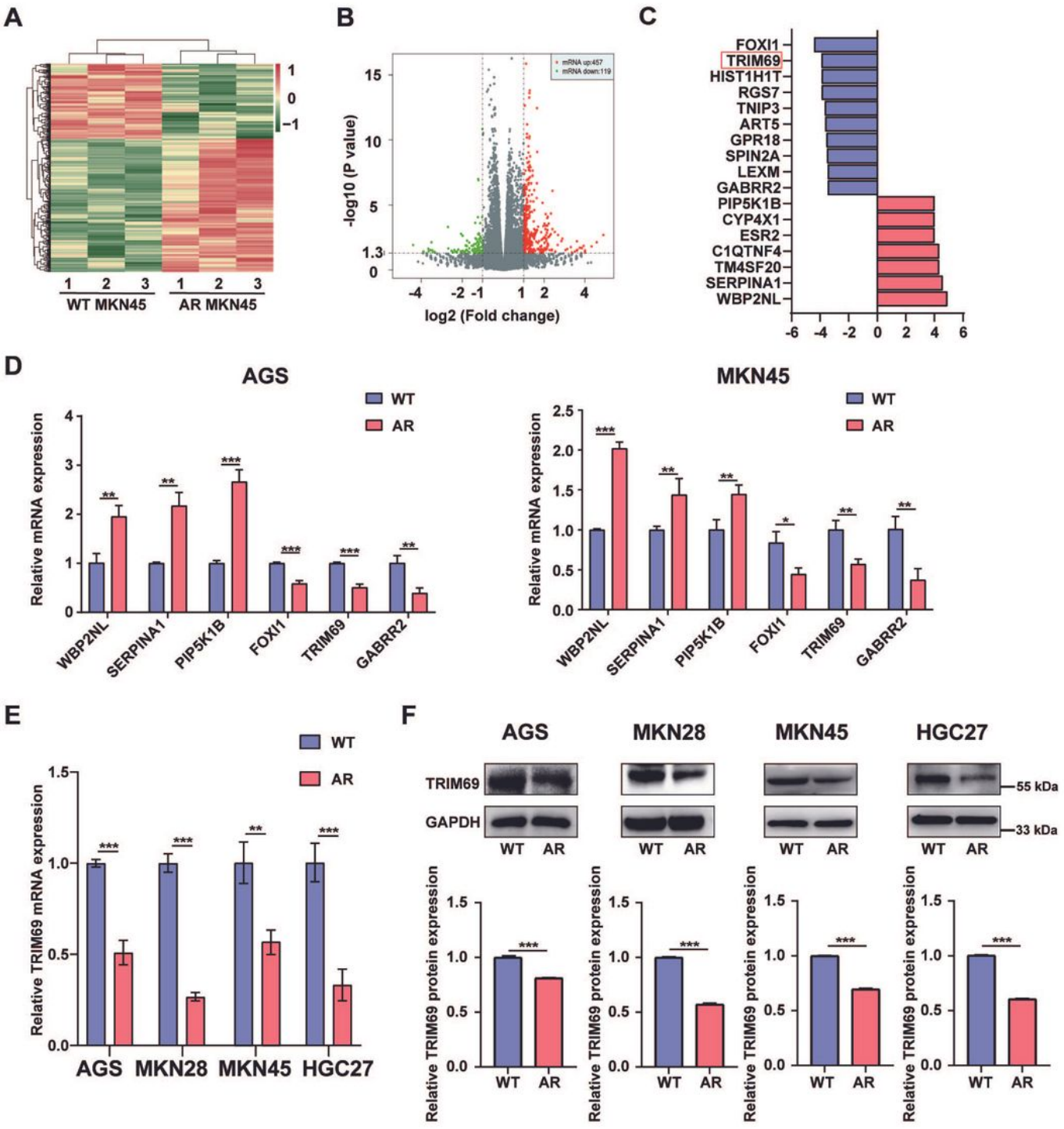

Figure 1

TRIM69 expression was low in anoikis-resistant GC cells.

(A-B) Heatmap and volcano plots showing the differential gene expression of WT MKN45 and anoikis-resistant (AR) MKN45 cells in RNA-seq data. **(C)** DEGs meeting the logarithmic fold change criteria (logFC > 4 and logFC < -3.4) were identified. **(D)** The expression of WBP2NL, SERPINA1, PIP5K1B, FOXI1, TRIM69 and GABRR2 was analyzedby RT—qPCR in WT and AR AGS and MKN45 cells. **(E)** The TRIM69 mRNA levels in WT and AR AGS, MKN28, MKN45 and HGC27 cells were measured by RT—qPCR. **(F)** The TRIM69 protein levels in WT and AR AGS, MKN28, MKN45 and HGC27 cells were measured by western blotting. GAPDH served as a loading control. Each experiment was performed in triplicate. The data are presented as the means ± SD and were analyzed by Student's *t* test (**p*< .05, ***p*< .01, ****p*< .001).

Figure 2

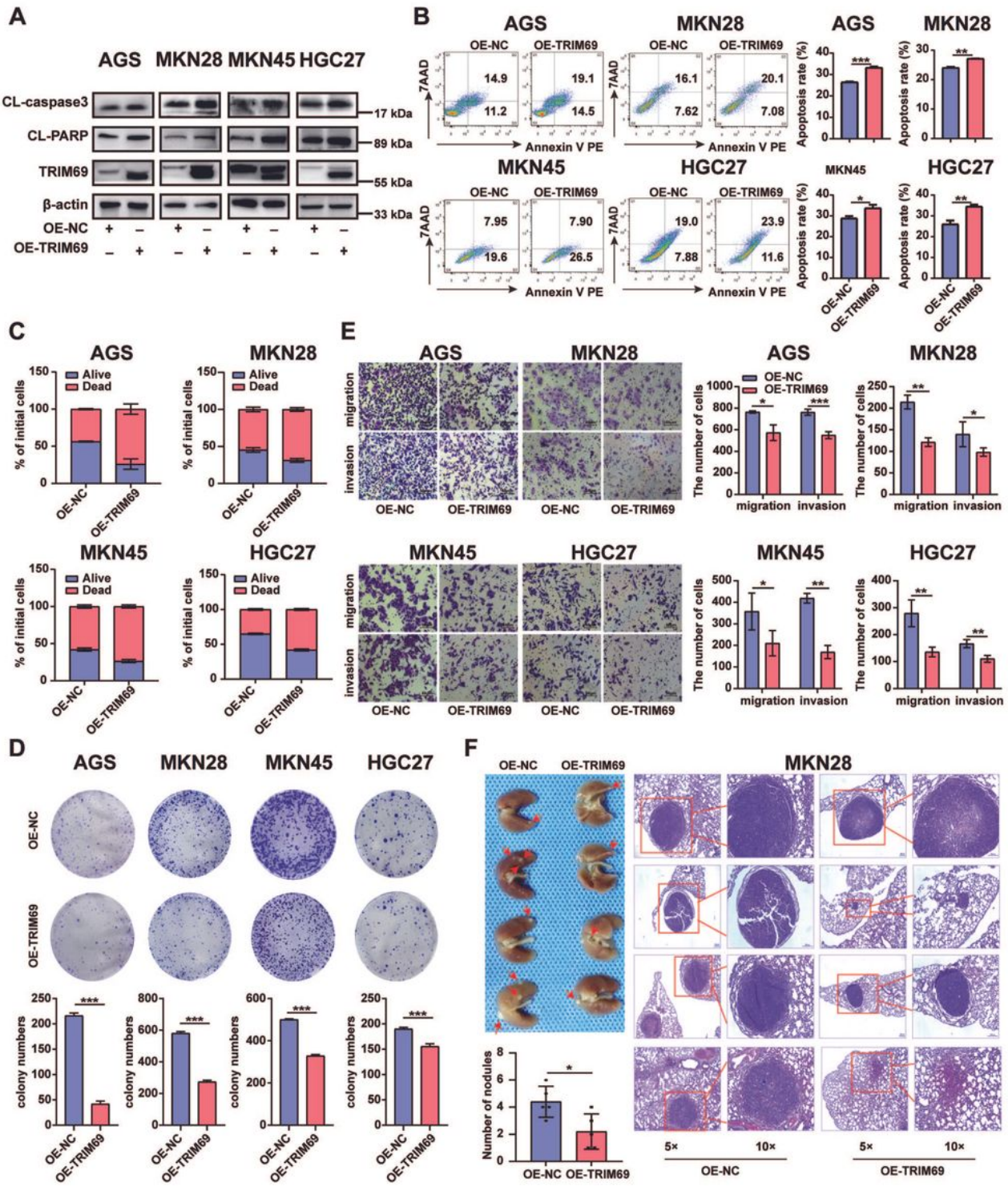

Figure 2

TRIM69 suppressed the anoikis resistance and metastasis of GC cells *in vitro* and *in vivo*.

(A) The protein levels of cleaved caspase3, cleaved PARP and TRIM69 in TRIM69-overexpressing (OE-TRIM69) AGS, MKN28, MKN45 and HGC27 cells. β-Actin served as a loading control. **(B)** Flow cytometry was used to measure the apoptosis rate of negative control-overexpressing (OE-NC) and OE-TRIM69 GC

cells in suspension culture. **(C)** Cell viability was determined by a trypan blue exclusion assay in OE-NC and OE-TRIM69 GC cells in suspension culture. **(D)** A colony formation assay was used to confirm the effects of OE-TRIM69 on the proliferative capacity of GC cells in low-serum medium (1% FBS). **(E)** Transwell assays were performed to determine the effects of TRIM69 overexpression on the migration and invasion abilities of GC cells. Scale bar, 50 μm. **(F)** The effects of TRIM69 overexpression on the lung metastasis of MKN28 cells *in vivo*. Lungs were observed for metastatic nodules on the surface and stained with H&E for histological analysis; the arrows indicate metastatic nodules. Representative photographs and H&E staining images are shown (n = 5 mice per group). Each experiment was performed in triplicate. The data are presented as the means ± SD and were analyzed by Student's *t*test (**p*< .05, ***p*< .01, ****p*< .001).

Figure 3

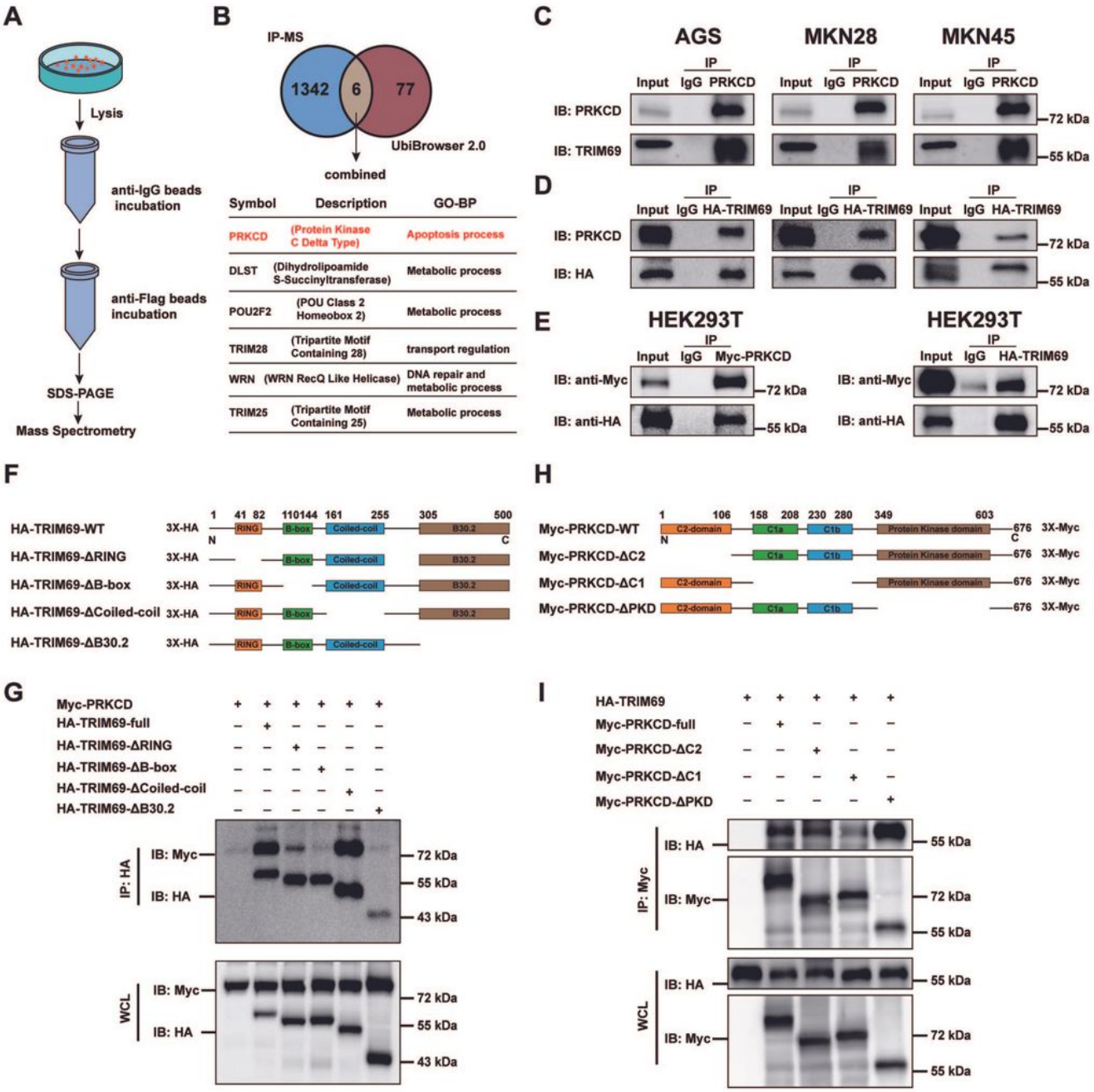

Figure 3

TRIM69 directly interacted with PRKCD.

(A) Interacting proteins that coimmunoprecipitated with TRIM69 in Flag-TRIM69 MKN45 cells were identified by mass spectrometry. **(B)** Six putative substrate proteins targeted by TRIM69 were predicted by theUbiBrowser 2.0 website and mass spectrometry results. **(C)** Immunoprecipitation and western blot

analysis showed the endogenous interaction between TRIM69 and PRKCD in AGS, MKN28 and MKN45 cells. **(D)** HA-tagged TRIM69 interacted with endogenous PRKCD in AGS, MKN28 and MKN45 cells. **(E)** The interaction of TRIM69 and PRKCD in HEK293T cells transfected with HA-TRIM69 and Myc-PRKCD. **(F)** Schematic of the full-length and truncated TRIM69 sequences. **(H)** Schematic of the full-length and truncated PRKCD sequences. **(G, I)** Co-IP assay results showing the binding regions between TRIM69 (G) and PRKCD (I). Each experiment was performed in triplicate. The data are presented as the means ± SD and were analyzed by Student's *t* test (**p*< .05, ***p*< .01, ****p*< .001).

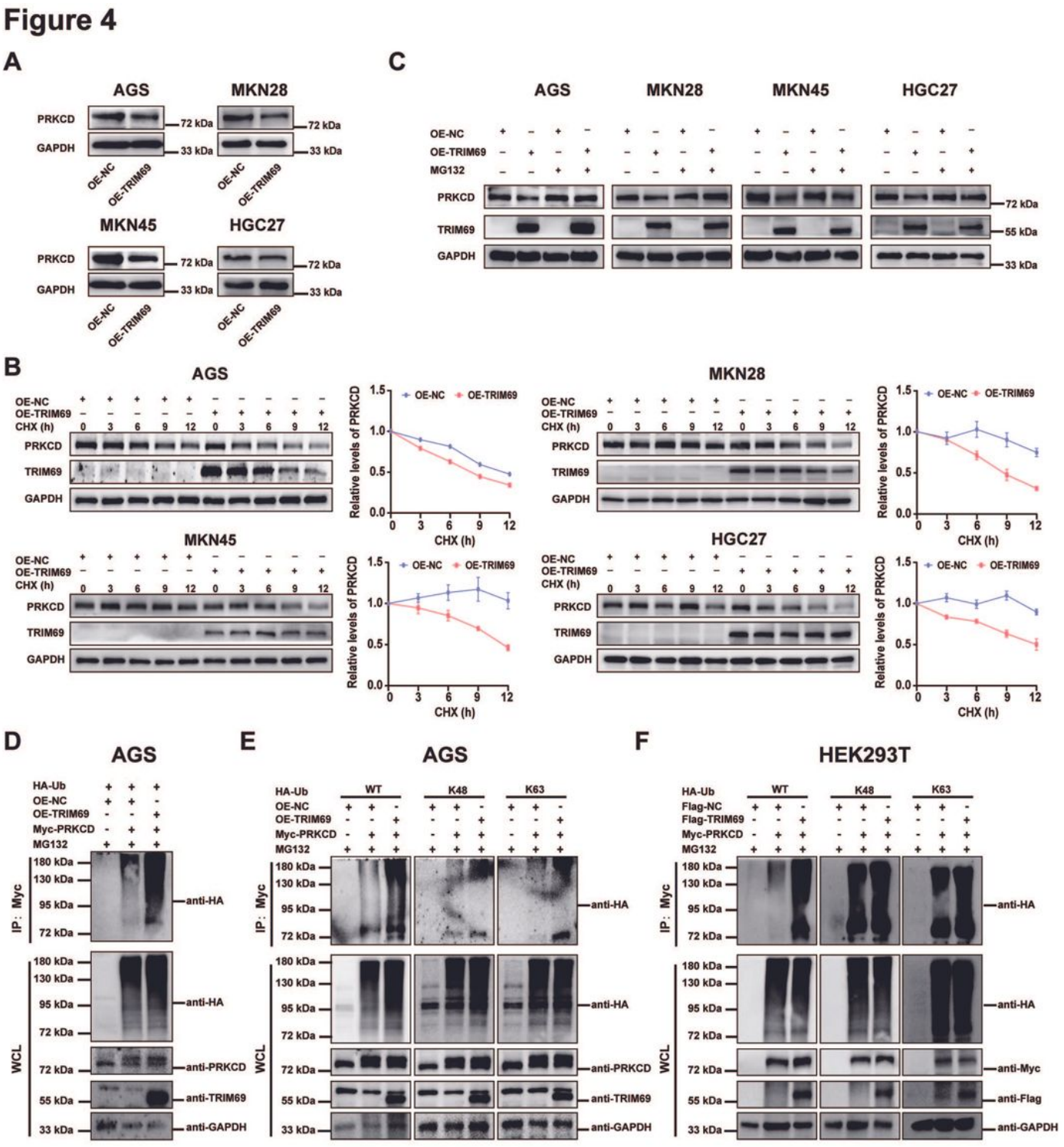

Figure 4

TRIM69 directly degraded PRKCD via the ubiquitin—proteasome pathway.

(A)PRKCD protein levels were measured by western blottingin OE-NC and OE-TRIM69 GC cells. GAPDH expression was used for normalization. **(B)** Western blot analysis showed the stability of the PRKCD protein in OE-NC and OE-TRIM69 GC cells in the presence of cycloheximide (CHX, 40 μM) for the indicated times. GAPDH expression was used for normalization. **(C)** Western blot analysis showed the expression level of the PRKCD protein in OE-NC and OE-TRIM69 GC cells treated with the proteasome inhibitor MG132. Cells were treated with 20 μM MG132 for 6 h. GAPDH expression was used for normalization. **(D)** TRIM69-overexpressing AGS cells were cotreatedwith the HA-Ubiquitin plasmid, Myc-PRKCD plasmid and MG132. PRKCD ubiquitination was detected by immunoprecipitation with anti-Myc beads and analyzed by immunoblotting with the indicated antibodies. **(E-F)**TRIM69-overexpressing AGS cells were cotransfected with Myc-PRKCD and different linkage types of HA-Ubiquitin (WT, K48, K63), and were then treated with MG132 (E); HEK293T cells were cotransfected with Myc-PRKCD, different linkage types of HA-Ubiquitin (WT, K48, K63) and Flag-TRIM69 and were then treated with MG132 (F). Cell lysates were immunoprecipitated with anti-Myc beads and analyzed by immunoblotting with the indicated antibodies. Each experiment was performed in triplicate. The data are presented as the means ± SD and were analyzed by Student's *t* test (**p*< .05, ***p*< .01, ****p*< .001).

Figure 5

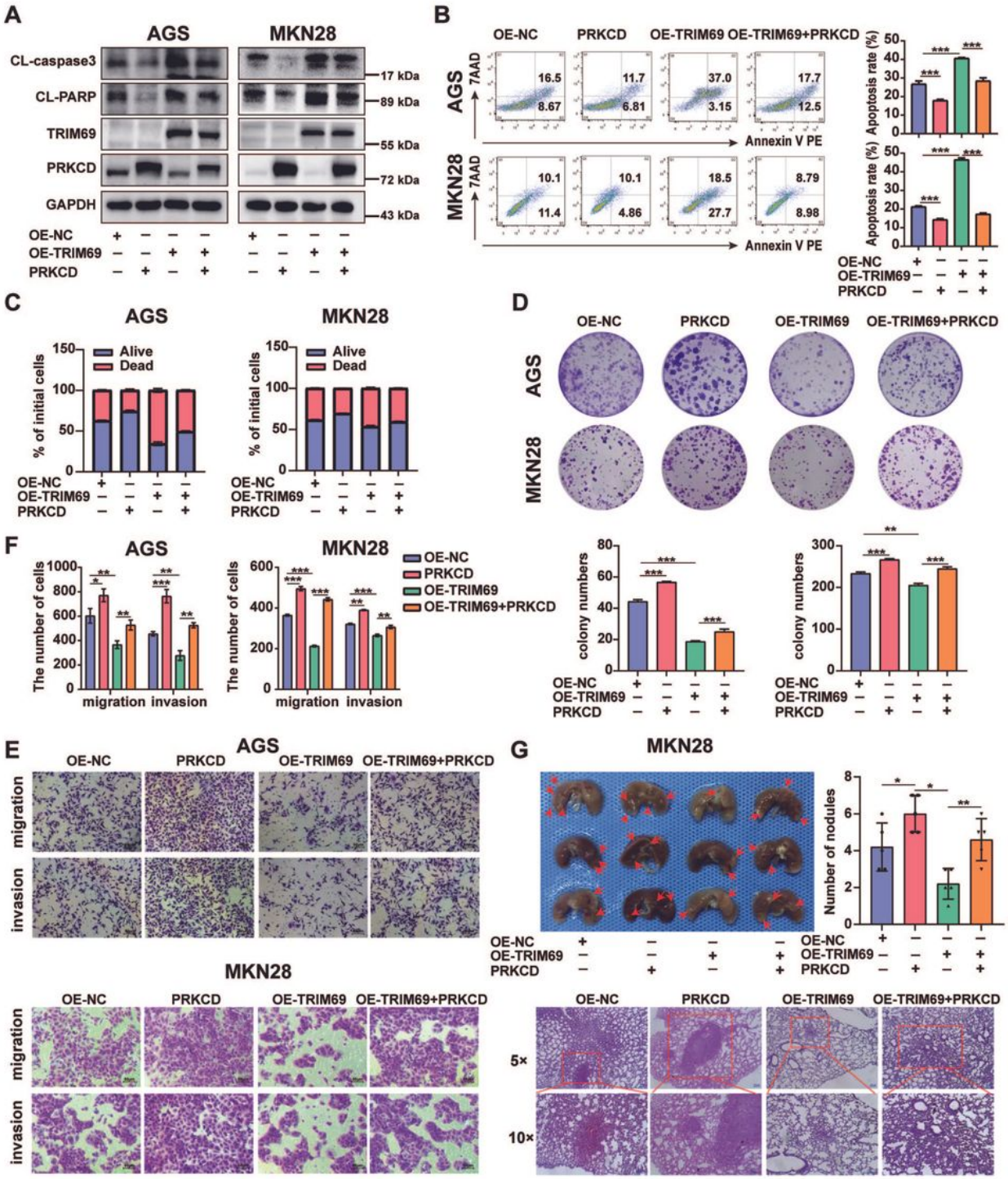

Figure 5

PRKCD is required for TRIM69 to suppress the anoikis resistance and metastasis of GC cells.

(A) Western blotting was used to measure the levels of cleaved caspase3, cleaved PARP, PRKCD and TRIM69 in OE-NC and OE-TRIM69 AGS and MKN28 cells treated with the PRKCD plasmid. GAPDH served as the loading control. **(B)** Flow cytometric analysis of the apoptosis rate of OE-NC and OE-TRIM69 AGS

and MKN28 cells treated with the PRKCD plasmid in suspension culture. **(C)** A Trypan blue exclusion assay was used to measure the viability of OE-NC and OE-TRIM69 AGS and MKN28 cells treated with the PRKCD plasmid. **(D)** A colony formation assay was used to determine theproliferative capacity of OE-NC and OE-TRIM69 AGS and MKN28 cells treated with the PRKCD plasmid in low-serum medium (1% FBS). **(E-F)** Transwell migration and invasion assays and the corresponding statistical results in OE-NC and OE-TRIM69 AGS and MKN28 cells treated with the PRKCD plasmid. Scale bar, 50 μm. **(G)** Treatment with the PRKCD expression plasmid reversed the effects of TRIM69 overexpression on the metastasis of MKN28 cells *in vivo*. Lungs were observed for metastatic nodules on the surface and stained with H&E for histological analysis; thearrows indicate metastatic nodules. Representative photographs and H&E staining images areshown (n = 5 mice per group). Scale bar, 100 μm. Each experiment was performed in triplicate. The data are presented as the means ± SD and were analyzed by Student's *t* test (**p*< .05, ***p*< .01, ****p*< .001).

Figure 6

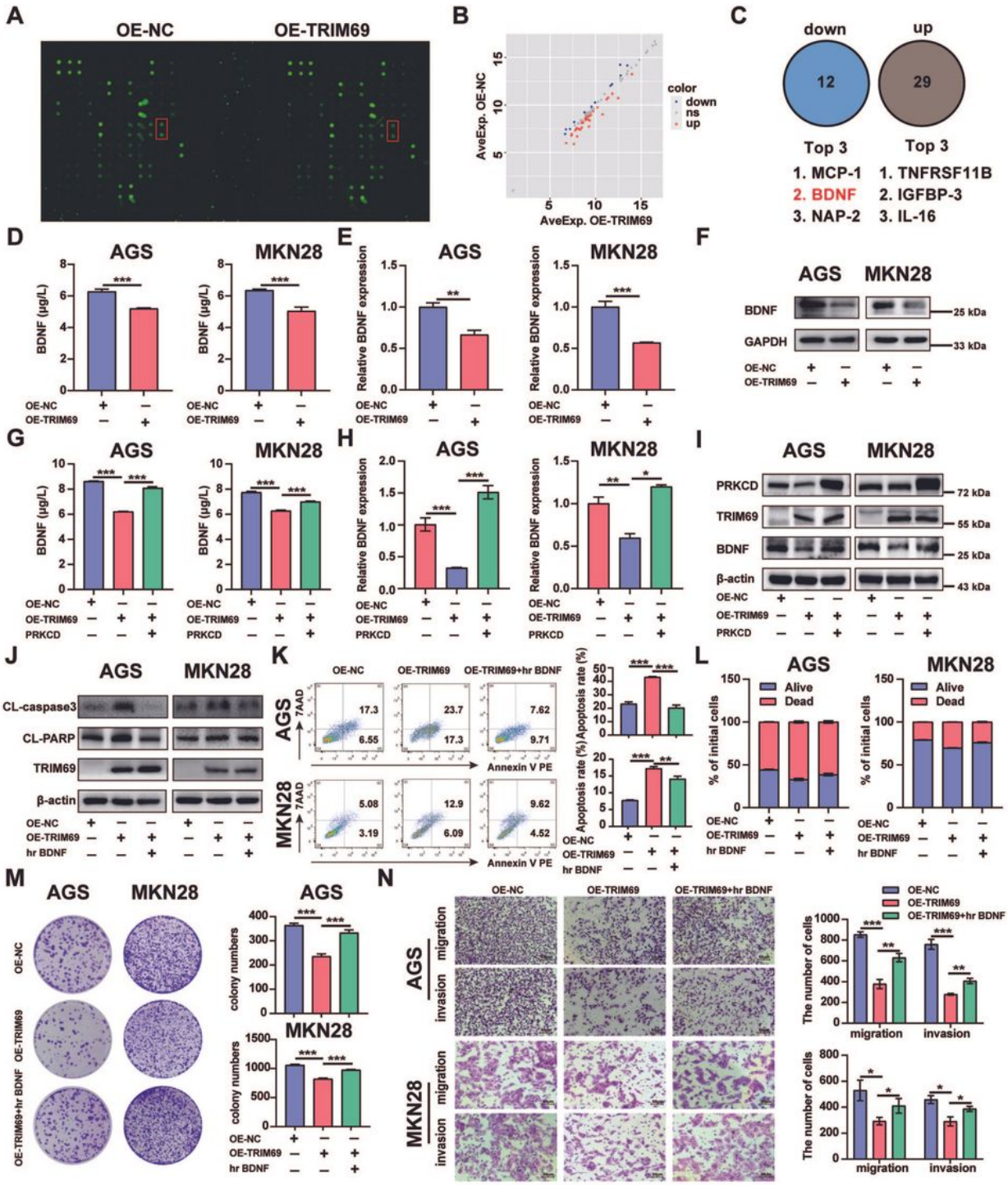

Figure 6

The TRIM69/PRKCD axis inhibited anoikis resistance and metastasis via BDNF in GC cells.

(A) A Human Cytokine Array G5 was used to identify the differentially expressed cytokines in the supernatants of OE-NC and OE-TRIM69 MKN45 cells. **(B)** Volcano plots showing the differentially expressed cytokines in the supernatants of OE-NC and OE-TRIM69 MKN45 cells. **(C)** Up- and

downregulatedcytokines areshown. **(D)** ELISA was used to measure BDNF expression in OE-NC and OE-TRIM69 AGS and MKN28 cell supernatants. **(E)** The BDNF mRNA level was measured by RT—qPCR in OE-NC and OE-TRIM69 AGS and MKN28 cells. **(F)** The BDNF protein level was measured by western blotting in OE-NC and OE-TRIM69 AGS and MKN28 cells. GAPDH served as the loading control. **(G)** ELISA was used to measure BDNF expression in the supernatants of OE-NC and OE-TRIM69 AGS and MKN28 cells after treatment with the PRKCD plasmid. **(H-I)** BDNF mRNA (H) and protein (I) levels in OE-NC and OE-TRIM69 AGS and MKN28 cells after treatment with the PRKCD plasmid. **(J)** Western blotting was used to measure the levels of cleaved caspase-3, cleaved PARP and TRIM69 in OE-NC and OE-TRIM69 AGS and MKN28 cells treated with hr BDNF. **(K)** Flow cytometric analysis ofthe apoptosis rate of OE-NC and OE-TRIM69 AGS and MKN28 cells treated with hr BDNF in suspension culture. **(L)** A Trypan blue exclusion assay was used to measure the viability of OE-NC and OE-TRIM69 AGS and MKN28 cells treated with hr BDNF in suspension culture.**(M)** Colony formation assay of the proliferative capacity of OE-NC and OE-TRIM69 AGS and MKN28 cells treated with hr BDNF in low-serum medium (1% FBS). **(N)** Transwell migration and invasion assays of OE-NC and OE-TRIM69 AGS and MKN28 cells treated with hr BDNF. Scale bar, 50 μm. Each experiment was performed in triplicate. The data are presented as the means ± SD and were analyzed by Student's *t* test (**p*< .05, ***p*< .01, ****p*< .001).

Figure 7

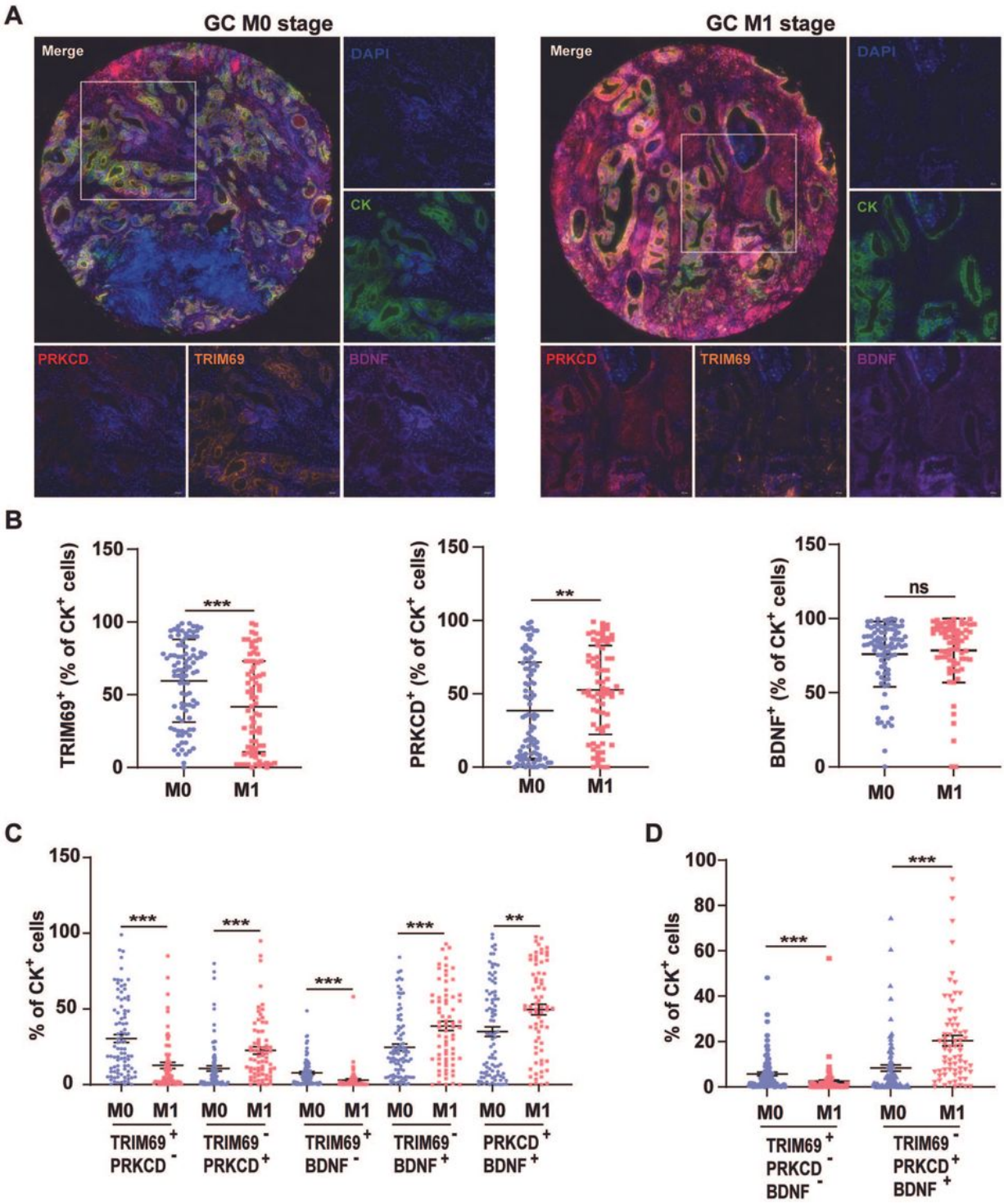

Figure 7

The proportion of TRIM69$^-$PRKCD$^+$BDNF$^+$ cells was positively associated with metastasis in GC patients.

(A) Representative images of TRIM69 (orange), PRKCD (red), BDNF (purple) and cytokeratin (CK, green) staining in GC tissue sections. **(B)** The percentages of TRIM69$^+$, PRKCD$^+$ and BDNF$^+$ tumor cells in nonmetastatic (M0) and metastatic (M1) GC tissues. **(C)** The percentages of TRIM69$^+$PRKCD$^-$, TRIM69$^-$

PRKCD^{+}, TRIM69^{+}BDNF^{-}, TRIM69^{-}BDNF^{+} and PRKCD^{+}BDNF^{+} tumor cells in M0 and M1 GC tissues. **(D)** The percentages of TRIM69^{+}PRKCD^{-}BDNF^{-} and TRIM69^{-}PRKCD^{+}BDNF^{+} tumor cells in M0 and M1 GC tissues. The data are presented as the means ± SEM and were analyzed by Student's *t* test (***p*< .01, ****p*< .001).

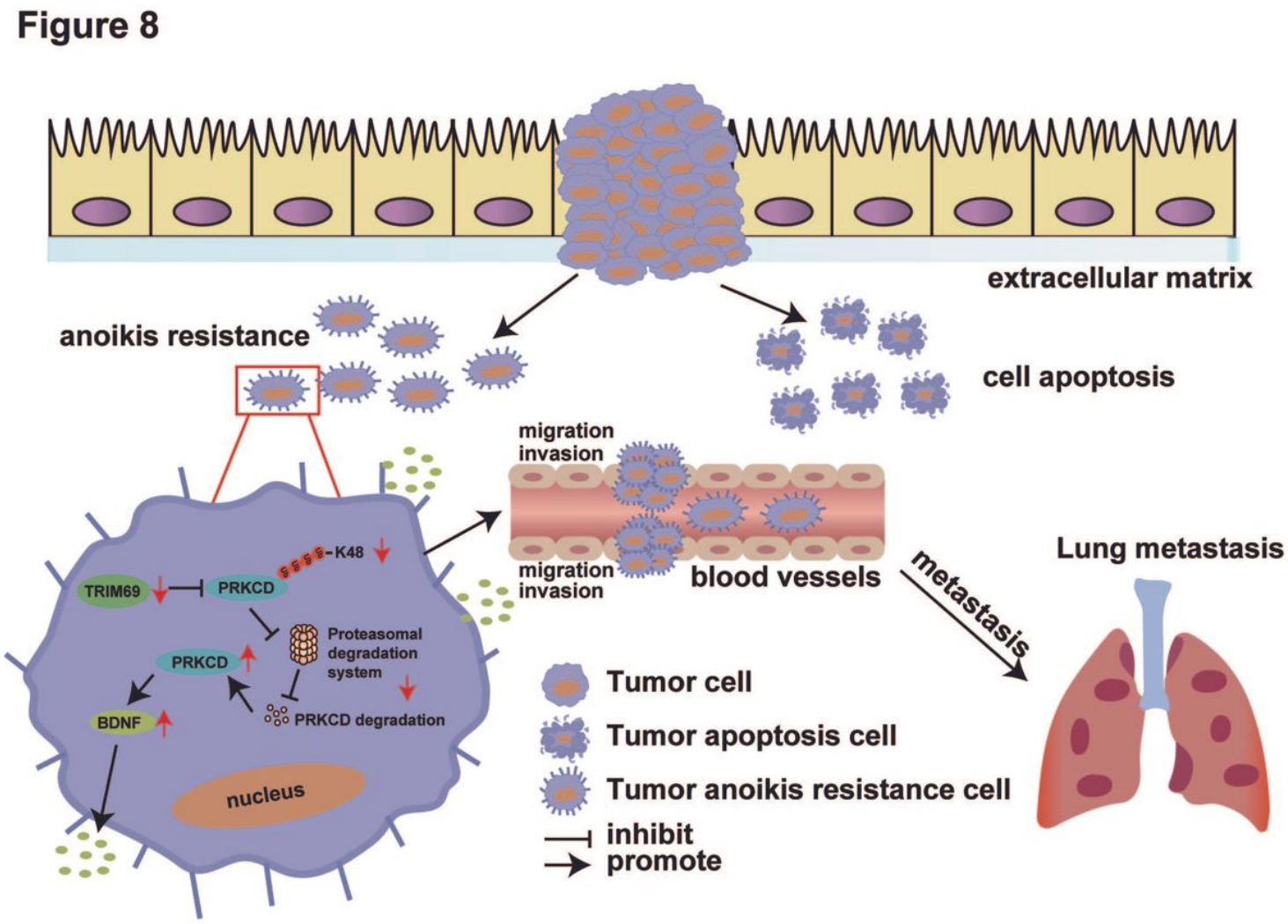

Figure 8

The mechanisms by whichTRIM69 suppresses GC anoikis resistance and metastasis.

Schematic diagram showing the regulatory mechanisms of the TRIM69/PRKCD/BDNF axis in anoikis resistance and metastasis in GC

Supplementary Files

This is a list of supplementary files associated with this preprint. Click to download.

- SupplementaryMaterialsandMethods.docx

- SupplementaryTables.docx
- SupplementaryFiguresandLegends.docx